

NASA/TM—1998-208656



Emittance Theory for Cylindrical Fiber Selective Emitter

Donald L. Chubb
Lewis Research Center, Cleveland, Ohio

Prepared for the
Fourth Conference on Thermophotovoltaic Generation of Electricity (TPV4)
sponsored by the National Renewable Energy Laboratory
Denver, Colorado, October 11–14, 1998

National Aeronautics and
Space Administration

Lewis Research Center

November 1998

Available from

NASA Center for Aerospace Information
7121 Standard Drive
Hanover, MD 21076
Price Code: A03

National Technical Information Service
5285 Port Royal Road
Springfield, VA 22100
Price Code: A03

EMITTANCE THEORY FOR CYLINDRICAL FIBER SELECTIVE EMITTER

Donald L. Chubb
National Aeronautics and Space Administration
Lewis Research Center
Cleveland, Ohio 44135

ABSTRACT

A fibrous rare earth selective emitter is approximated as an infinitely long cylinder. The spectral emittance, ϵ_λ , is obtained by solving the radiative transfer equations with appropriate boundary conditions and uniform temperature. For optical depths, $K_R = \alpha_\lambda R$, where α_λ is the extinction coefficient and R is the cylinder radius, greater than 1 the spectral emittance is nearly at its maximum value. There is an optimum cylinder radius, R_{opt} , for maximum emitter efficiency, η_E . Values for R_{opt} are strongly dependent on the number of emission bands of the material. The optimum radius decreases slowly with increasing emitter temperature, while the maximum efficiency and useful radiated power increase rapidly with increasing temperature.

INTRODUCTION

Fibrous rare earth oxide selective emitters for thermophotovoltaic (TPV) applications have been of research interest for several years. Nelson (1) began working with fibrous emitters in the 1980's. In addition fibrous emitters are being developed at Quantum Group (2) and the Auburn Space Power Institute (3). This paper develops the emittance theory for a fibrous emitter by approximating the emitter as an infinitely long cylinder. Since the fibrous emitters consist of bundles of 1 to 10 μm diameter fibers this theory does not include the effects of the reflectance that occurs when radiation leaves a fiber and enters an adjoining fiber. The whole bundle of fibers is being approximated as a continuous cylinder. If the fibers are closely packed and the reflectance at the interface between a fiber and the medium in the voids between fibers is small, then the error resulting from the approximation should be small.

The spectral emittance of the cylinder is obtained by solving the radiative transfer equation with appropriate boundary conditions. Knowing the spectral emittance allows the emitter efficiency to be calculated. As an example, emitter efficiency is calculated for an erbium-holmium aluminum garnet and thulium aluminum garnet ($\text{Tm}_3\text{Al}_5\text{O}_{12}$) which are being studied at NASA Lewis.

TEMPERATURE OF EMITTING CYLINDER

As pointed out earlier (4), temperature drop across a planar or film type emitter causes a major reduction in the spectral emittance in the emission band of a selective emitter. However, in most cases for a cylindrical emitter there will be a negligible temperature drop. This can be seen by considering the steady state energy equation for an infinite cylinder with no internal heat generation and thermal conductivity, k_{th} , and where we assume the temperature, T , and radiation flux, Q , depend only on the radial coordinate, r .

$$r \left[k_{th} \frac{dT}{dr} - Q \right] = \text{constant} \quad (1)$$

In order to avoid the term in brackets being singular at $r = 0$ it must vanish for all r . Thus at all r the conduction and radiation fluxes balance.

$$k_{th} \frac{dT}{dr} = Q \quad (2)$$

In other words, for all steady state conditions all the thermal energy being conducted into the cylinder at the outer radius, $r = R$, leaves the cylinder as radiation.

The radiation flux, Q , will always be less than the blackbody flux $\sigma_{sb} T^4$, where $\sigma_{sb} = 5.67 \times 10^{-12} \text{ w/cm}^2 \text{K}^4$ is the Stefan Boltzmann constant. Therefore, define the following dimensionless variables.

$$\bar{Q} = \frac{Q}{\sigma_{sb} T_s^4} \quad \bar{T} = \frac{T}{T_s} \quad \bar{r} = \frac{r}{R} \quad (3)$$

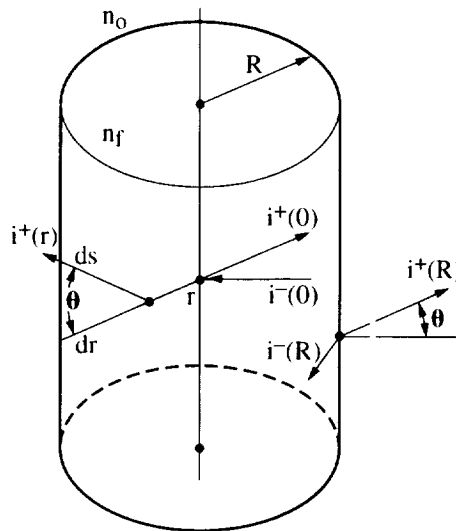
Where T_s is the temperature at $r = R$. In this case equation (2) becomes the following.

$$\frac{d\bar{T}}{d\bar{r}} = \gamma \bar{Q} \quad (4)$$

Where γ is the ratio of the radiation flux to the thermal conduction flux.

$$\gamma = \frac{\sigma_{sb} T_s^4}{k_{th} \frac{T_s}{R}} = \frac{\sigma_{sb} T_s^3 R}{k_{th}} \quad (5)$$

For the ceramic materials used in most selective emitters, $k_{th} \geq 0.01 \text{ w/cmK}$. Also, for TPV applications $T_s \leq 2000\text{K}$. Therefore, $\gamma \leq 4.5R(\text{cm})$. So that if $R < 0.1 \text{ cm}$ it is a reasonable approximation to neglect the right hand side of equation (4) and obtain the result $\bar{T} = \text{constant}$ ($T = T_s$). If $\gamma \ll 1$ for a film or planar emitter then a linear temperature variation results (4) rather than a uniform temperature. For the cylinder emittance calculation that follows, a uniform temperature is assumed.



n_f = index of refraction of cylinder
 n_o = index of refraction of surroundings
 $\cos\theta \, ds = dr$

FIGURE 1. Schematic of emitting cylinder.

SPECTRAL EMITTANCE OF CYLINDER

The spectral emittance is defined as follows.

$$\epsilon_\lambda \equiv \frac{q_\lambda(R)}{e_{bs}(\lambda, T_s)} \quad (6)$$

Where $q_\lambda(R)$ is the radiation flux leaving the cylinder at $r = R$ and $e_{bs}(\lambda, T_s)$ is the blackbody emissive power where λ is wavelength and T_s is the cylinder temperature.

$$e_{bs}(\lambda, T_s) = \pi i_{bs}(\lambda, T_s) = \frac{2\pi hc_0^2}{\lambda^5 [\exp(hc_0/\lambda k T_s) - 1]} \quad (7)$$

Appearing in equation (7) is the blackbody intensity $i_{bs}(\lambda, T_s)$, w/cm² nm steradian, Planck's constant, h , Boltzmann's constant, k , and the vacuum speed of light, c_0 . The radiation flux, $q_\lambda(R)$, is obtained by solving the radiation transfer equations for the intensities, $i_\lambda^+(R)$, and $i_\lambda^-(R)$. Where $i_\lambda^+(R)$ is the intensity moving in the +R direction and $i_\lambda^-(R)$ is the intensity moving in the -R direction as shown in figure 1. Assuming the intensities depend only on the radial coordinate leads to transport equations for $i_\lambda^+(R)$ and $i_\lambda^-(R)$ identical to the planar case (5). These equations are written in terms of the optical depth, K , rather than the coordinate, r .

$$K = \alpha_\lambda r \quad (8a)$$

$$K_R = \alpha_\lambda R \quad (8b)$$

Where α_λ is the extinction coefficient, assumed independent of r , and is the sum of the absorption coefficient, a_λ , and the scattering coefficient σ_λ .

$$\alpha_\lambda = a_\lambda + \sigma_\lambda \quad (9)$$

The boundary conditions that must be applied are the following. At $r = K = 0$, from symmetry conditions.

$$i_\lambda^+(0) = i_\lambda^-(0) \quad \text{at } K = 0 \quad (10a)$$

At $r = R$ or $K = K_R$ the intensity moving in the -R direction is equal to the reflected intensity.

$$i_\lambda^-(K_R) = \rho_{f_0} i_\lambda^+(K_R) \quad \text{at } K = K_R \quad (10b)$$

Where ρ_{f_0} is the reflectance at the cylinder outer radius, R . At $r = R$ total reflectance occurs for certain angles of incidence, θ . At an interface between a material with a index of refraction, n_i , and a material with index of refraction, n_j , where $n_i > n_j$, radiation moving from i into j with angles of incidence $\theta > \theta_M$, where θ_M is given by Snell's Law will be totally reflected. Since $n_f > n_o$, for the cylinder-air interface we have the following result for the reflectance, ρ_{f_0} .

$$\rho_{f_0} = 1 \quad \text{for } \theta \geq \theta_M \quad \text{where } \mu_M^2 \equiv \cos^2 \theta_M = 1 - \left(\frac{n_o}{n_f} \right)^2 \quad (11a)$$

For the case where $\theta < \theta_M$ ($\mu > \mu_M$) we approximate ρ_{f_0} by the reflectance for normal incidence (6).

$$\rho_{f0} = \left(\frac{n_f - n_o}{n_f + n_o} \right)^2 \theta < \theta_M \quad (\mu > \mu_M) \quad (11b)$$

Once the intensities $i_{\lambda}^+(K_R, \theta)$ and $i_{\lambda}^-(K_R, \theta)$ are obtained the radiation flux, $q_{\lambda}(K_R)$, can be calculated.

$$q_{\lambda}(K_R) = q_{\lambda}^+(K_R) - q_{\lambda}^-(K_R) \quad (12)$$

$$q_{\lambda}^+(K_R) = 2\pi \int_{\theta=0}^{\pi/2} i_{\lambda}^+(K_R, \theta) \cos \theta \sin \theta d\theta = 2\pi \int_0^1 i_{\lambda}^+(K_R, \mu) \mu d\mu \quad (13)$$

$$q_{\lambda}^-(K_R) = -2\pi \int_{\theta=\pi/2}^{\pi} i_{\lambda}^-(K_R, \theta) \cos \theta \sin \theta d\theta = 2\pi \int_0^1 i_{\lambda}^-(K_R, \mu) \mu d\mu \quad (14)$$

Solution of the radiative transfer equations for $q_{\lambda}(K_R)$ is presented in (5) for the film or planar case with a linear temperature variation through the film and for no scattering ($\sigma_s = 0$ in eq. (9)). Results for the uniform temperature cylinder can be obtained from these results by setting $\epsilon_{fs} = 0$ ($\rho_{fs} = 1$) and $\Delta T = 0$ in equations (33) to (36) of reference (5). When this is done the following result is obtained for the spectral emittance.

$$\epsilon_{\lambda} = \frac{n_o^2(1 - \rho_{f0}) \left[1 - 4E_3(K_R) \right]}{1 - 4E_3(K_R) \left[\rho_{f0}E_3(K_R) + \mu_M^2(1 - \rho_{f0})E_3\left(\frac{K_R}{\mu_M}\right) \right]} \quad (15)$$

uniform temperature and no scattering

Appearing in equation (15) is the exponential integral $E_3(x)$ defined as follows.

$$E_n(x) = \int_0^1 z^{n-2} \exp\left(-\frac{x}{z}\right) dz \quad (16)$$

The reflectance, ρ_{f0} , is given by equation (11b) and μ_M is given by equation (11a).

As equations (15) and (11) indicate, for no scattering the spectral emittance of a uniform temperature cylinder depends on the optical depth, K_R , and indices of refraction, n_f and n_o . For single crystal materials, such as rare earth doped yttrium aluminum garnet (YAG), scattering should be negligible. However, for polycrystalline rare earth oxides such as those being considered in references (1) to (3) scattering should be significant. In those cases equation (15) will overestimate the spectral emittance.

Consider ϵ_{λ} for the two limiting conditions $K_R = 0$ and $K_R \rightarrow \infty$. The $K_R = 0$ case corresponds to a wavelength where the material is transparent. While the $K_R \rightarrow \infty$ case applies to an emission band of a selective emitter. Since $E_3(0) = 1/2$ and $\lim_{x \rightarrow \infty} E(x) = 0$, equation (15) yields the following:

$$\epsilon_{\lambda} = 0 \quad \text{for} \quad K_R = 0 \quad (17)$$

$$\lim_{K_R \rightarrow \infty} \epsilon_{\lambda} = n_o^2(1 - \rho_{f0}) \quad (18)$$

Equation (18) is the usual result for an opaque body emitting (or absorbing) in vacuum ($n_o = 1$).

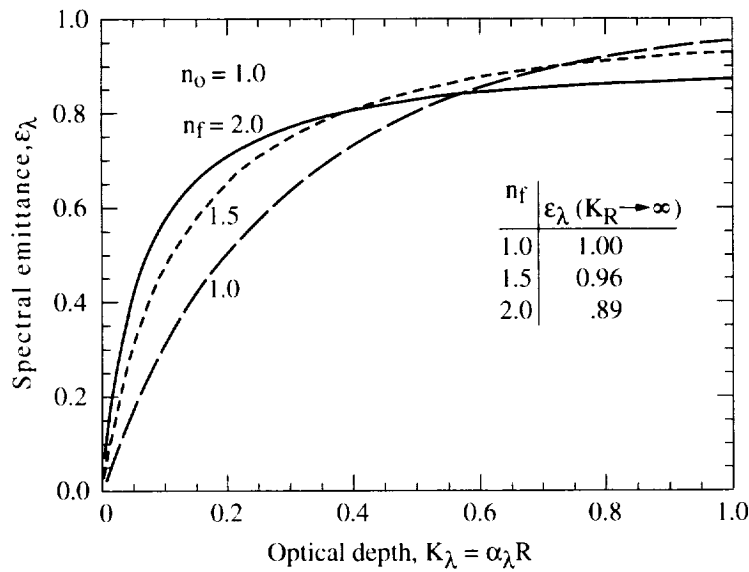


FIGURE 2. Spectral emittance for cylinder of radius, R , at a constant temperature, T_s , as a function of optical depth, $K_\lambda = \alpha_\lambda R$, where α_λ is the extinction coefficient and n_f is the cylinder index of refraction and n_o is the surrounding index of refraction.

In figure 2 the spectral emittance, ϵ_λ , using equation (15) is shown as a function of optical depth, K_R , for $n_o = 1$ and $n_f = 1, 1.5$ and 2.0 . As figure 2 shows ϵ_λ increases rapidly with K_R and reaches nearly its limiting value (eq. (18)) for $K_R = 1$. Notice also that for small K_R as n_f increases the spectral emittance rate of increase also increases. For most of the selective emitter materials, $1.5 \leq n_f \leq 2.0$.

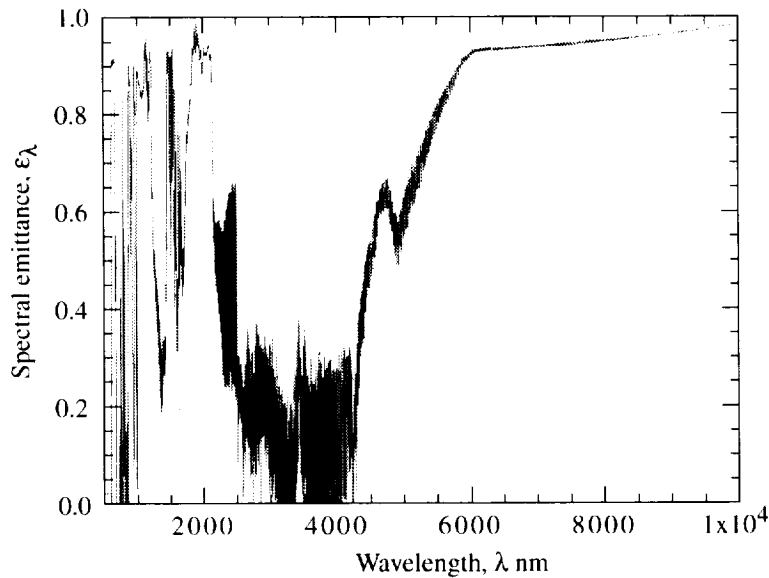


FIGURE 3. Theoretical spectral emittance of $\text{Er}_{0.3}\text{Ho}_{2.7}\text{Al}_5\text{O}_{12}$ cylinder of radius, $R = 0.4$ cm, calculated using measured extinction coefficient and index of refraction.

Once the extinction coefficient, α_λ , and index of refraction, n_λ , are known equation (15) can be used to calculate ϵ_λ . Figure 3 shows the calculated spectral emittance for an erbium-holmium aluminum garnet cylinder ($R = 0.4$ cm) with 10% erbium and 90% holmium, $\text{Er}_{0.3}\text{Ho}_{2.7}\text{Al}_5\text{O}_{12}$. This single crystal material is being considered for a film type selective emitter (5). The extinction coefficient and index of refraction were obtained from reference (5). Holmium has its main emission band centered at $\lambda \approx 2000$ nm with smaller bands centered at $\lambda \approx 1100, 890$ and 750 nm. Erbium has its main emission band centered at $\lambda \approx 1500$ nm with secondary bands centered at $\lambda \approx 1000, 800$ and 640 nm. All of these bands show up as regions of large emittance in figure 3. In the region $2000 < \lambda < 4500$ nm, $\text{Er}_{0.3}\text{Ho}_{2.7}\text{Al}_5\text{O}_{12}$ is nearly transparent ($\alpha_\lambda \rightarrow 0$) and thus ϵ_λ is small. The highly oscillatory result in this region results from numerical error in α_λ (5). For the region $\lambda > \lambda_c = 5000$ nm ϵ_λ becomes large again. This large ϵ_λ results from vibrational modes of the crystal lattice and is a characteristic of most rare earth selective emitter materials (1). We call the wavelength, λ_c , the long wavelength cutoff.

EMITTER EFFICIENCY

As a measure of the effectiveness of a selective emitter define the emitter efficiency as follows.

$$\eta_E \equiv \frac{\text{useful radiated power}}{\text{total radiated power}} = \frac{Q_b}{Q_T} = \frac{\int_0^{\lambda_g} q_\lambda(R) d\lambda}{\int_0^\infty q_\lambda(R) d\lambda} = \frac{\int_0^{\lambda_g} \epsilon_\lambda e_{bs}(\lambda, T_s) d\lambda}{\int_0^\infty \epsilon_\lambda e_{bs}(\lambda, T_s) d\lambda} \quad (19)$$

The numerator, Q_b , is the power radiated in the wavelength region $0 \leq \lambda \leq \lambda_g$. In a TPV system λ_g corresponds to the bandgap energy, $E_g = hc_0/\lambda_g$, of the PV cell. The denominator is the total radiated power, Q_T .

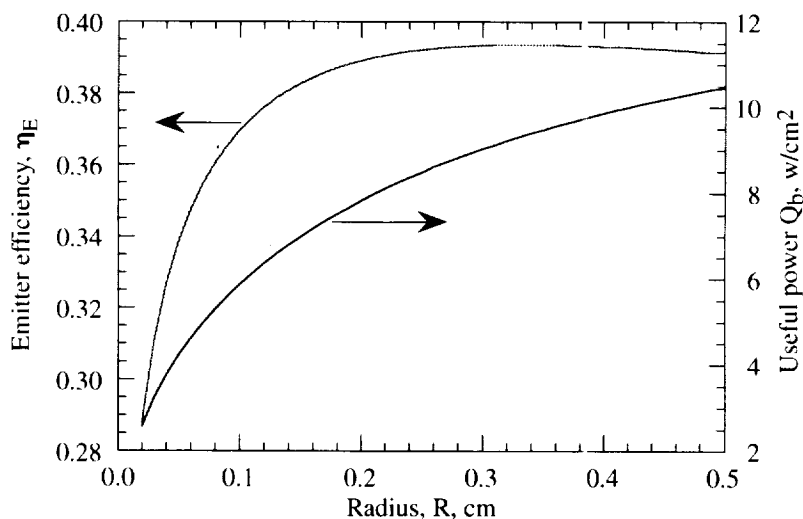


FIGURE 4. Emitter efficiency, η_E , and useful power, Q_b , as a function of cylinder radius, R , at emitter temperature, $T_s = 1700$ K for $\text{Er}_{0.3}\text{Ho}_{2.7}\text{Al}_5\text{O}_{12}$.

Consider how η_E will behave as a function of the cylinder radius, R . As figure 2 shows, ϵ_λ increases rapidly with optical depth, $K_R = \alpha_\lambda R$. Therefore, for the emission bands and the long wavelength region (large α_λ and $\lambda < \lambda_g$ or $\lambda > \lambda_c$) ϵ_λ will quickly approach its limiting value as R increases from zero. However, for the regions between the emission bands and the long wavelength cutoff (small α_λ and $\lambda_1 < \lambda < \lambda_c$) the spectral emittance will increase more slowly to its limiting value as R increases from zero. Thus, the numerator of equation (19), Q_b , will rapidly rise from zero to its limiting value as R increases from zero. At the same time, the denominator, Q_T , will

increase more slowly and will continue increasing with R while the numerator is increasing at a much lower rate. As a result, there will be an optimum radius, R_{opt} , that will yield maximum η_{EMAX} . This is illustrated in figure 4 for $Er_{0.3}Ho_{2.7}Al_5O_{12}$ where $\lambda_g = 2200$ nm ($E_g = 0.56$ eV) was chosen for use in equation (19) and $T_s = 1700$ K. As can be seen, η_E rises rapidly to η_{EMAX} and then decreases slowly for $R > R_{opt}$. Also shown in figure 4 is the useful power radiated, Q_b . As can be seen, Q_b rises rapidly and then begins to level off. For $T_s = 1700$ K the optimum radius is $R_{opt} = 0.34$ cm. It should be mentioned that for radii of this magnitude the uniform temperature assumption becomes questionable. In figures 5(a) and (b) R_{opt} , $\eta_E(R_{opt})$ and $Q_b(R_{opt})$ are shown as functions of T_s . Both $\eta_E(R_{opt})$ and $Q_b(R_{opt})$ increase significantly with temperature while R_{opt} decreases only 25 percent in going from $T_s = 1200$ to 2000 K. The large increase in η_E results because the maximum value of the blackbody emissive power, $e_{bs}(\lambda, T_s)$, shifts to shorter wavelengths as T_s increases. Therefore, Q_b increases faster than Q_T as T_s increases. The useful power, Q_b , increases at least as T_s^4 .

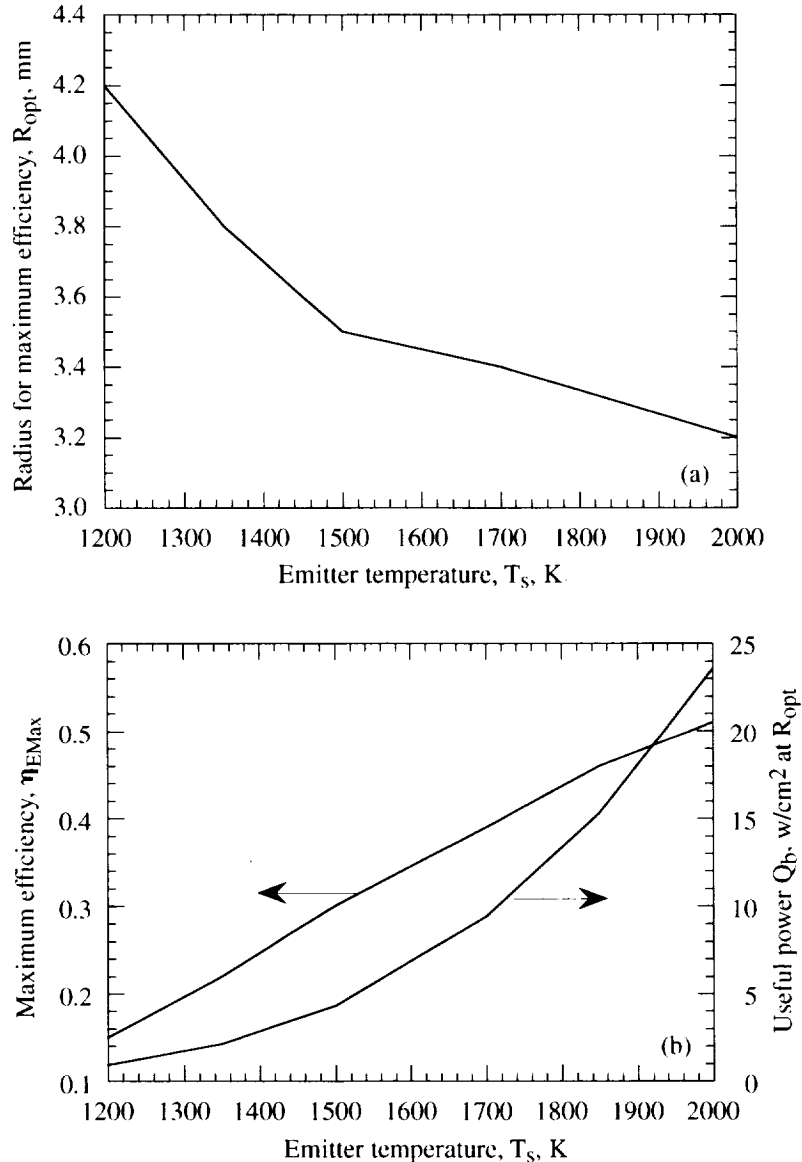


FIGURE 5. Optimum radius, R_{opt} , maximum efficiency, η_{EMax} , and useful power, Q_b , at $R = R_{opt}$ as functions of emitter temperature, T_s , for $Er_{0.3}Ho_{2.7}Al_5O_{12}$. (a) Optimum radius, R_{opt} . (b) Maximum efficiency and useful power.

Now consider thulium aluminum garnet, $\text{Tm}_3\text{Al}_5\text{O}_{12}$, as a cylindrical selective emitter. Thulium has its main emission band centered at $\lambda \approx 1700$ nm with smaller bands centered at $\lambda \approx 1200, 800$ and 700 nm. Thus compared to $\text{Er}_{0.3}\text{Ho}_{2.7}\text{Al}_5\text{O}_{12}$, which has 8 emission bands and thus a large region of high ϵ_λ for $\lambda < \lambda_g$, $\text{Tm}_3\text{Al}_5\text{O}_{12}$ has a much smaller high emittance region for $\lambda < \lambda_g$. For $\text{Tm}_3\text{Al}_5\text{O}_{12}$, $\lambda_g = 1900$ nm was chosen. Just as for $\text{Er}_{0.3}\text{Ho}_{2.7}\text{Al}_5\text{O}_{12}$, thulium aluminum garnet has large emittance for $\lambda > \lambda_c = 5000$ nm.

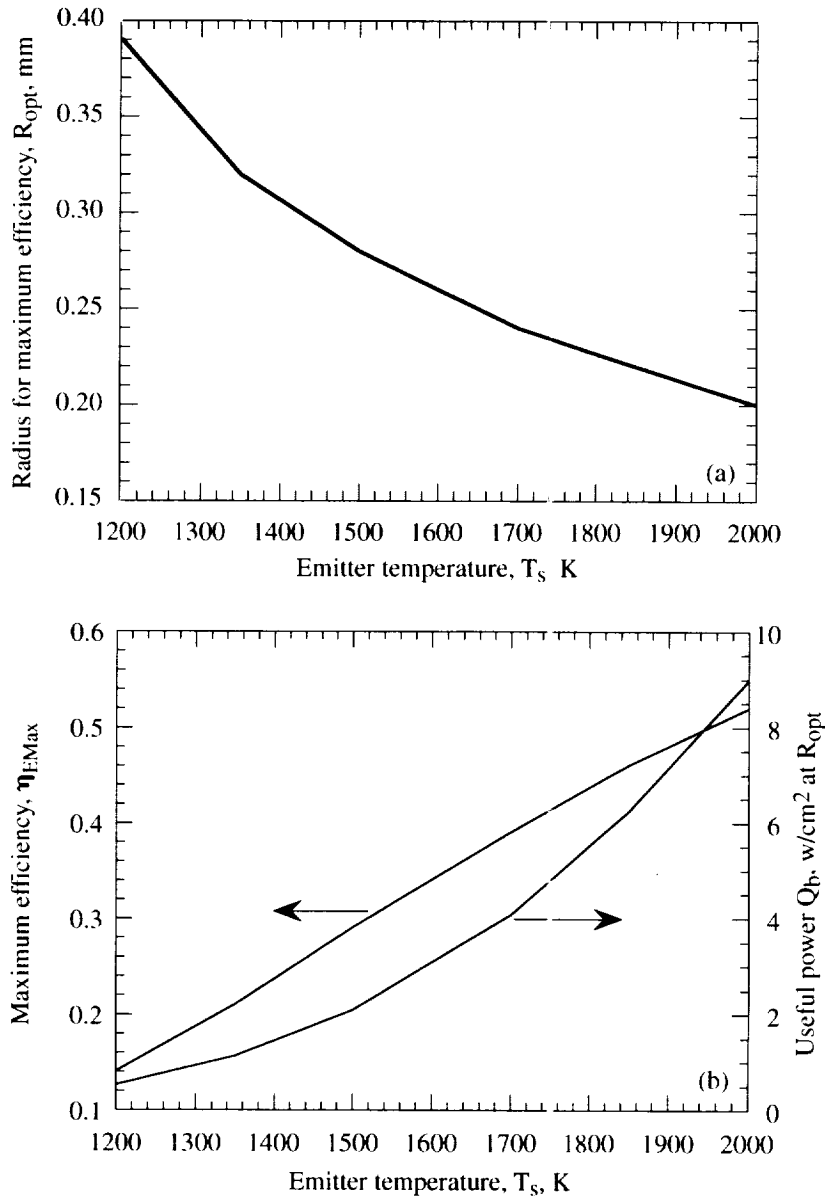


FIGURE 6. Optimum radius, R_{opt} , maximum efficiency, $\eta_{E\text{Max}}$, and useful power, Q_b , at $R = R_{\text{opt}}$ as functions of emitter temperature, T_s , for $\text{Tm}_3\text{Al}_5\text{O}_{12}$. (a) Optimum radius, R_{opt} . (b) Maximum efficiency and useful power.

In figure 6(a) and (b), R_{opt} , $\eta_E(R_{\text{opt}})$ and $Q_b(R_{\text{opt}})$ are shown as functions of T_s for $\text{Tm}_3\text{Al}_5\text{O}_{12}$. These results were calculated using measured values for α_λ and $n_f(5)$. The first thing to notice is that R_{opt} for $\text{Tm}_3\text{Al}_5\text{O}_{12}$ is much smaller than R_{opt} for $\text{Er}_{0.3}\text{Ho}_{2.7}\text{Al}_5\text{O}_{12}$. This occurs because thulium aluminum garnet has a smaller region of large emittance than erbium-holmium aluminum-garnet, as mentioned above. Therefore, the majority of Q_b results from emission in the main emission band centered at $\lambda \approx 1900$ nm where $\alpha_\lambda \approx 30 \text{ cm}^{-1}$. Thus when $R \approx 0.3$ mm, $K_R \approx 1$

and ϵ_λ will be near its maximum value (fig. 2). As a result, Q_b will also be near its maximum and thus η_E will be a maximum. Therefore, we expect that R_{opt} will occur near 0.3 mm for thulium aluminium garnet. Figure 6(a) substantiates this result.

Comparing figures 5(b) and 6(b) we see that the emitter efficiencies are nearly the same for $Er_{0.3}Ho_{2.7}Al_5O_{12}$ and $Tm_3Al_5O_{12}$. However, the useful power, Q_b , is much larger for $Er_{0.3}Ho_{2.7}Al_5O_{12}$. This occurs for two reasons. First of all, erbium-holmium aluminum garnet has a much larger region of large emittance for $\lambda < \lambda_g$ than thulium aluminum garnet. Secondly, $\lambda_g = 1900$ nm for thulium aluminum garnet whereas $\lambda_g = 2200$ nm for erbium-holmium aluminum garnet. Thus more of the spectrum is included in Q_b for $Er_{0.3}Ho_{2.7}Al_5O_{12}$.

An important point about selective emitters is brought out by comparing figures 5(b) and 6(b). That is, η_E and useful power, Q_b , do not behave in the same manner. Increasing Q_b by adding more emission bands, as in the case of $Er_{0.3}Ho_{2.7}Al_5O_{12}$, does not mean that η_E will increase.

CONCLUSION

Most fibrous rare earth selective emitters consist of bundles of 1 to 10 μ m diameter bundles. In this study that bundle has been approximated as an infinite cylinder. From the solution to the radiative transfer equations the spectral emittance of the cylindrical emitter was calculated. Several conclusions can be made about the cylindrical rare earth selective emitters.

1. For most rare earth selective emitters the temperature is uniform through the cylinder.
2. When the optical depth $K_R = \alpha_\lambda R \geq 1$ the spectral emittance is nearly a maximum.
3. There is an optimum value for the radius, R_{opt} , which yields maximum emitter efficiency.
4. R_{opt} strongly depends on the emitter material. For an emitter with only a single strong emission band R_{opt} is the order of 0.1 mm, whereas for an emitter with many emission bands R_{opt} is the order of 1 mm.
5. R_{opt} decreases slowly with increasing emitter temperature.
6. The maximum efficiency, η_{EMAX} , and useful power, Q_b , increase significantly with temperature.

REFERENCES

1. Nelson, R.E., "Thermophotovoltaic Emitter Development," presented at the First NREL Conference on Thermophotovoltaic Generation of Electricity, AIP Proc. 321, 80.
2. Holmquist, G.A., "TPV Power Source Development for an Unmanned Undersea Vehicle," presented at the First NREL Conference, AIP Proc. 321, 308.
3. Adair, P.L. and Rose, M.F., "Composite Emitters for TPV Systems," presented at the First NREL Conference, AIP Proc. 321, 245.
4. Chubb, D.L., Good, B.S., Clark, E.B. and Chen, Z., "Effect of Temperature Gradient on Thick Film Selective Emitter Emittance," presented at the Third NREL Conference on Thermophotovoltaic Generation of Electricity, AIP Proc. 401, 293.
5. Chubb, D.L., Pal, A.T., Patton, M.O. and Jenkins, P.P., "Rare Earth Doped High Temperature Ceramic Selective Emitters," to be published in the *Journal of the European Ceramic Society*, also NASA/TM—1998-208491.
6. Siegel, R. and Howell, J.R., "Thermal Radiation Heat Transfer," 2nd edition, Washington, D.C., Hemisphere, 1981, Ch. 4.

REPORT DOCUMENTATION PAGE

Form Approved
OMB No. 0704-0188

Public reporting burden for this collection of information is estimated to average 1 hour per response, including the time for reviewing instructions, searching existing data sources, gathering and maintaining the data needed, and completing and reviewing the collection of information. Send comments regarding this burden estimate or any other aspect of this collection of information, including suggestions for reducing this burden, to Washington Headquarters Services, Directorate for Information Operations and Reports, 1215 Jefferson Davis Highway, Suite 1204, Arlington, VA 22202-4302, and to the Office of Management and Budget, Paperwork Reduction Project (0704-0188), Washington, DC 20503.

1. AGENCY USE ONLY (Leave blank)	2. REPORT DATE November 1998	3. REPORT TYPE AND DATES COVERED Technical Memorandum	
4. TITLE AND SUBTITLE Emittance Theory for Cylindrical Fiber Selective Emitter		5. FUNDING NUMBERS WU-632-1A-1A-00	
6. AUTHOR(S) Donald L. Chubb		8. PERFORMING ORGANIZATION REPORT NUMBER E-11378	
7. PERFORMING ORGANIZATION NAME(S) AND ADDRESS(ES) National Aeronautics and Space Administration Lewis Research Center Cleveland, Ohio 44135-3191		9. SPONSORING/MONITORING AGENCY NAME(S) AND ADDRESS(ES) National Aeronautics and Space Administration Washington, DC 20546-0001	
9. SPONSORING/MONITORING AGENCY NAME(S) AND ADDRESS(ES) National Aeronautics and Space Administration Washington, DC 20546-0001		10. SPONSORING/MONITORING AGENCY REPORT NUMBER NASA TM-1998-208656	
11. SUPPLEMENTARY NOTES Prepared for the Fourth Conference on Thermophotovoltaic Generation of Electricity (TPV4) sponsored by the National Renewable Energy Laboratory, Denver, Colorado, October 11-14, 1998. Responsible person, Donald L. Chubb, organization code 5410, (216) 433-2242.			
12a. DISTRIBUTION/AVAILABILITY STATEMENT Unclassified - Unlimited Subject Categories: 20 and 76 This publication is available from the NASA Center for AeroSpace Information, (301) 621-0390.		12b. DISTRIBUTION CODE Distribution: Nonstandard	
13. ABSTRACT (Maximum 200 words) A fibrous rare earth selective emitter is approximated as an infinitely long cylinder. The spectral emittance, ϵ_λ , is obtained by solving the radiative transfer equations with appropriate boundary conditions and uniform temperature. For optical depths, $K_R = \alpha_\lambda R$, where α_λ is the extinction coefficient and R is the cylinder radius, greater than 1 the spectral emittance is nearly at its maximum value. There is an optimum cylinder radius, R_{opt} , for maximum emitter efficiency, η_E . Values for R_{opt} are strongly dependent on the number of emission bands of the material. The optimum radius decreases slowly with increasing emitter temperature, while the maximum efficiency and useful radiated power increase rapidly with increasing temperature.			
14. SUBJECT TERMS Thermophotovoltaics; Selective emitter		15. NUMBER OF PAGES 15	
		16. PRICE CODE A03	
17. SECURITY CLASSIFICATION OF REPORT Unclassified	18. SECURITY CLASSIFICATION OF THIS PAGE Unclassified	19. SECURITY CLASSIFICATION OF ABSTRACT Unclassified	20. LIMITATION OF ABSTRACT